

Phase transition in a many-electron gas in a two-dimensional polar-semiconductor quantum well

Ashok Chatterjee

School of Physics, University of Hyderabad, Central University Post Office, Hyderabad 500 134, India

Shreekantha Sil

Saha Institute of Nuclear Physics, Solid State and Molecular Physics Division, Sector-1, Block-AF, Bidhannagar, Calcutta 700 064, India

(Received 18 May 1994)

We investigate the problem of an electron gas interacting with longitudinal-optical phonons in a two-dimensional polar-semiconductor quantum well for the entire range of the coupling parameter using the Feynman path-integral method and the random-phase approximation. We show that at a critical value of the electron concentration an optical polaron will undergo a transition from the localized state to a mobile state.

I. INTRODUCTION

With the development of modern fabrication techniques like molecular-beam epitaxy and metal-organic chemical-vapor deposition, it has now become possible to realize quasi-one-dimensional and two-dimensional electronic systems. Consequently, there has been a great deal of activity in recent years in the field of low-dimensional systems such as thin films, inversion layers, quantum wells, and heterojunction superlattices of polar semiconductors. These studies are important from the point of view of fundamental physics as well as for applications to electronic devices. The polaronic interaction plays an important role in determining the transport and other properties of these systems and has, therefore, been extensively studied in these materials both theoretically and experimentally (see Refs. 1–4 and references therein). Earlier theories¹ were, however, developed using the single polaron model of Fröhlich which neglects the electron-electron interaction completely. This would be a reasonably good model for low-carrier density systems like ionic crystals. But in semiconductor structures the carrier concentration is quite significant and so the Coulomb interaction between electrons can give rise to important many-body effects. Indeed the free-carrier screening was discussed long ago by Ehrenreich⁵ in the context of bulk polar semiconductors. Das Sarma² studied for the first time the screening effects on the polaronic interaction in a quasi-two-dimensional structure and showed that many-body effects would lead to an appreciable decrease in the polaron mass correction. Subsequently, this problem has been investigated by several authors³ using different types of screening. All these calculations were, however, based on weak-coupling approximations. In a recent paper,⁶ we performed an all coupling variational calculation to study the many-electron effect on the ground-state (GS) energy, effective mass and size of a polaron in a purely two-dimensional (2D) quantum well using the random-phase approximation (RPA).

This method was based on Huybrecht's modification⁷ of the Lee, Low, and Pines (LLP) canonical transformation technique,⁸ and is known to have certain disadvantages. Therefore, in the present paper, we investigate the same problem using the Feynman path-integral method which is the most elegant physical and mathematical approach providing at the same time the best GS solution for the entire range of the electron-phonon coupling constant α . Here, also, we include the many-electron screening effect within the framework of RPA and reestablish the same conclusion that there exists a critical carrier density (depending on α) below which the polaron will be in a self-trapped state and if the carrier density exceeds this value, it will make a transition to the delocalized state. The present calculation is, however, more rigorous and is, therefore, expected to yield quantitatively more accurate results.

II. FORMULATION

A system of an electron gas in 2D interacting with 2D optical phonons of dispersionless frequency ω_0 may be modeled (in Feynman units) by the Hamiltonian,

$$\mathcal{H} = -\frac{1}{2} \sum_j \vec{\nabla}_{\vec{\rho}_j}^2 - \sum_{i>j} v(\vec{\rho}_i - \vec{\rho}_j) + \sum_j b_{\vec{q}}^\dagger b_{\vec{q}} + \sum_j \sum_{\vec{q}} \left[i \left[\frac{\sqrt{2\pi\alpha}}{Aq} \right]^{1/2} e^{-i\vec{q}\cdot\vec{\rho}_j} b_{\vec{q}}^\dagger + \text{H.c.} \right], \quad (1)$$

where everything is dimensionless. $\vec{\rho}_j$ refers to the position vector of the j th electron, $b_{\vec{q}}^\dagger$ ($b_{\vec{q}}$) is the creation (annihilation) operator for a phonon of wave vector \vec{q} , $v(\vec{\rho}_i - \vec{\rho}_j)$ represents the Coulomb interaction between the i th and j th electrons, A stands for the surface area of the 2D material and α is the electron-phonon coupling constant in two dimensions. For a purely 2D material, α can be assumed to be given by an expression similar to that in 3D, while for the interaction of a surface electron with the surface-optical phonons on a bulk material, the

form of α has to be slightly modified (see Sil and Chatterjee¹). The electron-electron interaction term cannot be treated exactly, so we have to include its effect in some approximate way. We shall assume that the sole effect of the electron-electron interaction is to screen the electron-phonon coupling which is a reasonable approximation. The simplest way to include this screening is to use the Thomas-Fermi method which is, however, not a useful approach in two dimensions because the Thomas-Fermi screening parameter does not depend at all on the electronic density in two dimensions. Therefore, we treat the electron-electron interaction within the framework of the static RPA which has been shown to be quantitatively accurate in 3D (Ref. 5) and has also been successfully used in 2D by Xiaoguang, Peeters, and Devreese (1986) (Ref. 3) and Das Sarma and Mason (1985).³ In the static RPA scheme the effective Hamiltonian for an electron interacting with surface-optical phonons in the presence of other electrons of density N_s can be written as

$$H_{\text{eff}} = -\frac{1}{2}\nabla_{\vec{\rho}}^2 + \sum_{\vec{q}} b_{\vec{q}}^{\dagger} b_{\vec{q}} + \sum_{\vec{q}} \left[i \left(\frac{\sqrt{2}\pi\alpha}{Aq(\epsilon(q,0))^2} \right)^{1/2} \times e^{-i\vec{q}\cdot\vec{\rho}} b_{\vec{q}}^{\dagger} + \text{H.c.} \right], \quad (2)$$

where $\epsilon(q,0)$ is the static RPA dielectric function given by⁹

$$\epsilon(q,0) = \left[1 + \frac{q_{\text{FT}}}{q} \right], \quad \text{for } q < 2k_F \\ = \left[1 + \frac{q_{\text{FT}}}{q} \left\{ 1 - \left[1 - \left(\frac{2k_F}{q} \right)^2 \right]^{1/2} \right\} \right], \\ \text{for } q > 2k_F, \quad (3)$$

where q_{FT} is the Thomas-Fermi screening parameter, and k_F is the Fermi momentum. In Ref. 6, we have solved the model problem (2) using a variational method (LLP- H), which is a generalization of the LLP method⁸ as proposed by Huybrechts,⁷ in the context of the single polaron problem. In this method, we minimize the functional

$$J = \langle \Psi | H_{\text{eff}} - \vec{u} \cdot \vec{P} | \Psi \rangle, \quad (4)$$

where \vec{u} is a Lagrange multiplier to be identified as the polaron velocity and Ψ is a trial wave function, which we choose as

$$|\Psi\rangle = \frac{\lambda}{\sqrt{\pi}} \exp \left[-\frac{\lambda^2}{2} \rho^2 + i\vec{p}_0 \cdot \vec{\rho} \right] \exp \left[-ia \sum_{\vec{q}} \vec{q} \cdot \vec{\rho} b_{\vec{q}}^{\dagger} b_{\vec{q}} \right] \\ \times \exp \left[\sum_{\vec{q}} (f_{\vec{q}} b_{\vec{q}}^{\dagger} - f_{\vec{q}}^* b_{\vec{q}}) \right] |0\rangle, \quad (5)$$

where λ , a , \vec{p}_0 , and $f_{\vec{q}}$ are obtained variationally and $|0\rangle$ is the unperturbed zero-phonon state which satisfies $b_{\vec{q}}|0\rangle=0$ for all \vec{q} . The LLP- H method gives reasonably accurate results, but some confusing complications are known to arise in this scheme in the weak-coupling regime. Furthermore, we find that in this method the pola-

ron size is always infinity in the entire weak-coupling regime which is a little unrealistic. We, therefore, employ in the present paper the Feynman path-integral method (FPIM) to solve the effective model Hamiltonian (2).

In FPIM, one calculates the transformation function K for the electron going from the point $(\vec{\rho}_a, t_a)$ to $(\vec{\rho}_b, t_b)$ with the phonon system remaining in the GS. K is finally given by^{10,11}

$$K = \int_a^b \mathcal{D}\vec{\rho}(t) e^S, \quad (6)$$

where the classical action S is given by

$$S = -\frac{1}{2} \int \left[\frac{d\vec{\rho}}{dt} \right]^2 dt \\ + \frac{\pi\alpha}{\sqrt{2}A} \sum_{\vec{q}} \int \int \frac{dt ds}{[\epsilon(q,0)]^2} \frac{e^{i\vec{q}\cdot[\vec{\rho}(t)-\vec{\rho}(s)]}}{q} e^{-|t-s|}, \quad (7)$$

which is, however, not path integrable. Therefore, we choose, following Feynman, a nonlocal Gaussian action,

$$S_1 = -\frac{1}{2} \int \left[\frac{d\vec{\rho}}{dt} \right]^2 dt - \frac{1}{2} - C \int \int ds dt |\vec{\rho}(t) - \vec{\rho}(s)|^2 \\ \times e^{-\omega|t-s|}, \quad (8)$$

with ω and C are two variational parameters. Using the Feynman-Jensen inequality $\langle e^x \rangle \geq e^{\langle x \rangle}$, where x is a real function, we then obtain for the variational energy,

$$E_F = \frac{(v-\omega)^2}{2v} \\ - \frac{\alpha}{\sqrt{2}} \int_0^\infty \int_0^\infty \frac{dk dt}{[\epsilon(k,0)]^2} e^{-t} \\ \times \exp \left[\left\{ -\frac{(v^2-\omega^2)}{2v^2} (1-e^{-vt}) - \frac{\omega^2 t}{2v^2} \right\} k^2 \right]. \quad (9)$$

where $v^2 = \omega^2 + 4C/\omega$. Finally, the GS energy is obtained by minimizing (9) with respect to v and ω . In the weak-coupling limit, C is negligible and, therefore, the GS corresponds to a value of v which is nearly equal to ω . Writing $v = (1+\Delta)\omega$, where Δ is a small number, in Eq. (9) and taking the limit $\Delta \rightarrow 0$, we obtain the energy in the weak-coupling limit:

$$E_F^{\text{WC}} = -\frac{\alpha}{\sqrt{2}} \int_0^\infty \frac{dk}{(1+k^2/2)[\epsilon(k,0)]^2}, \quad (10)$$

which was earlier obtained by Xiaoguang, Peeters, and Devreese (1986) (Ref. 3) and is also identical to the weak-coupling LLP- H result.⁶ In the limit $N_s \rightarrow 0$, Eq. (10) gives, as expected, the well-known LLP energy. For the entire range of the coupling parameter, the minimization of (10) with respect to ω and v is done numerically. Results are shown in Fig. 1.

To calculate the effective mass for a slow polaron we consider, following Feynman, all paths from $(0,0)$ to $(u\tau, \tau)$, where τ is the time interval and u is an imaginary velocity. The corresponding transformation function for small displacement in the limit $\tau \rightarrow \infty$ is assumed to take

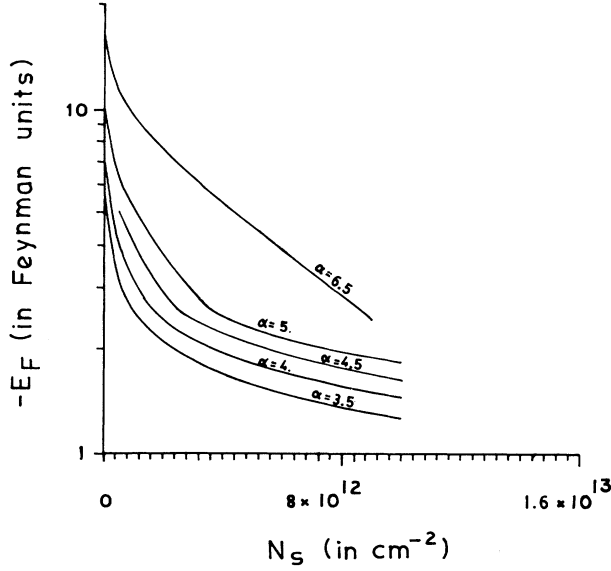


FIG. 1. $-E_F$ vs N_S , E_F , polaron GS energy; N_S , carrier concentration.

the following form:

$$K \sim e^{-[E_F(0) + \frac{1}{2}m_F^*u^2]\tau} = e^{-E_F(u)\tau}. \quad (11)$$

Thus, equating the total energy $E_F(u)$ to $E_F(0) + \frac{1}{2}m_F^*u^2$, we obtain the following expression for the effective mass:

$$m_F^* = 1 + \frac{\alpha}{2\sqrt{2}} \int_0^\infty \int_0^\infty \frac{dk dt}{[\epsilon(k,0)]^2} k^2 t^2 e^{-t} \times \exp \left\{ \left[-\frac{(v^2 - \omega^2)}{2v^3} (1 - e^{-vt}) - \frac{\omega^2 t}{2v^2} \right] k^2 \right\}, \quad (12)$$

which in the weak-coupling limit reduces to

$$m_F^* = 1 + \frac{\alpha}{2\sqrt{2}} \int_0^\infty \frac{dq}{\left[1 + \frac{q^2}{2}\right]^2 [\epsilon(q,0)]^2}, \quad (13)$$

which is again identical to the effective-mass result of Xiaoguang, Peeters, and Devreese (1986) (Ref. 3) and the weak-coupling limit of the LLP- H expression.⁶ For the entire range of α , the effective mass is obtained numerically and shown in Fig. 2.

To calculate the size of the polaron, we follow the method of Schultz.¹¹ Schultz has simulated the Feynman approximation by replacing the whole lattice by a second fictitious particle bound harmonically to the electron. The Lagrangian of such a model system is

$$L = \frac{1}{2} \left[\frac{d\vec{\rho}}{dt} \right]^2 + \frac{1}{2} M \left[\frac{d\vec{X}}{dt} \right]^2 - \frac{1}{2} K [\vec{\rho} - \vec{X}]^2 - U_0, \quad (14)$$

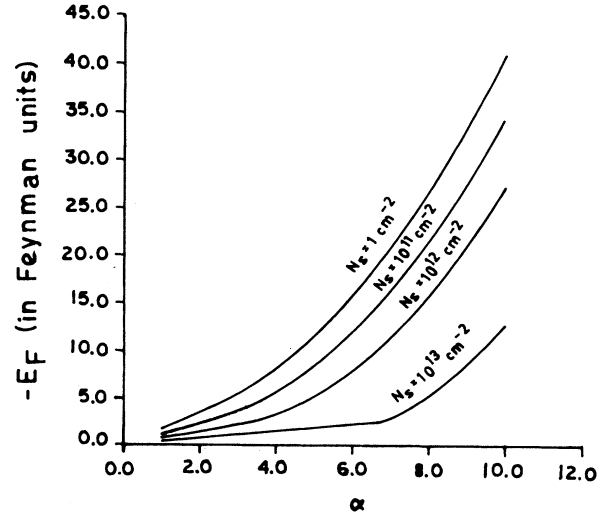


FIG. 2. $-E_F$ vs electron-phonon coupling constant (α) for $N_S = 1, 10^{11}, 10^{12}, 10^{13} \text{ cm}^{-2}$.

where M and \vec{X} refer to the fictitious second particle and U_0 is a constant to be so chosen as to make the model system have the same energy E_F . The correspondence of the model (14) with the Feynman action becomes exact (except for some effects which are unimportant for large time) if the following identifications are made:

$$M = \{(v^2/\omega^2) - 1\}; \quad K = (v^2 - \omega^2). \quad (15)$$

In the center-of-mass coordinates, we can write (14) as

$$L = \frac{1}{2}(1+M) \left[\frac{d\vec{R}}{dt} \right]^2 + \frac{1}{2} \left[\frac{M}{1+M} \right] \left[\frac{d\vec{\rho}_1}{dt} \right]^2 - \frac{1}{2} K \rho_1^2, \quad (16)$$

where $\vec{\rho}_1 = (\vec{X} - \vec{\rho})$ and $\vec{R} = (M\vec{X} + \vec{\rho})/(M+1)$. The Hamiltonian corresponding to (16) is

$$H = \frac{1}{2}(1+M) \left[\frac{d\vec{R}}{dt} \right]^2 + \frac{1}{2} \mu \left[\frac{d\vec{\rho}_1}{dt} \right]^2 + \frac{1}{2} K \rho_1^2, \quad (17)$$

where $\mu = M/(1+M) = (v^2 - \omega^2)/v^2$. The quantum-mechanical Hamiltonian for the Feynman polaron is, thus, given by

$$H_F = \frac{p^2}{2\mu} + \frac{1}{2} K \rho_1^2, \quad (18)$$

which is exactly soluble. The GS wave function of this Hamiltonian is given by

$$\Phi(\vec{\rho}_1) = \left[\frac{\mu K}{\pi^2} \right]^{1/4} \exp \left[-\frac{\sqrt{\mu K}}{2} \rho_1^2 \right], \quad (19)$$

and the radius of the Feynman polaron is defined as the root mean square distance of the electron from the fictitious particle. Thus, the size (R) of the polaron is given by

$$R = [\langle \Phi(\vec{\rho}_1) | \rho_1^2 | \Phi(\vec{\rho}_1) \rangle]^{1/2} = [v/(v^2 - \omega^2)]^{1/2}, \quad (20)$$

III. NUMERICAL RESULTS AND DISCUSSION

Let us now discuss our numerical results for all values of α . In Fig. 1, we plot the GS energy as a function of the electronic density, N_s . It is evident from the figure that many-body effects inhibit the polaronic interaction significantly. One can, furthermore, observe that the variation of the GS energy with N_s is quite rapid, when N_s is less than a critical value, N_{sc} which, however, depends on α . In Fig. 2, we show the variation of the GS energy with α for different carrier concentrations ($N_s = 1, 10^{11}, 10^{12}$, and 10^{13} cm^{-2}). We observe that for low values of α , the GS energy is essentially linear in α while for large α , it varies quite rapidly with α . Thus, there seems to exist a critical coupling constant α_c below which the polaron is in the weak-coupling regime. This is more clearly shown in Figs. 3 and 4, in which we have also plotted the LLP-H results⁷ for the sake of comparison. For low values of α , the agreement between the FPIM and the LLP-H results is excellent, but for intermediate and strong coupling, the FPIM clearly yields better results. One may note that the value of α_c increases as the electron concentration increases.

Figure 5 gives the variation of the effective mass (m_F^*) of the polaron as a function of N_s for different values of α ($\alpha = 1, 3, 3.5, 4, 4.5, 5, 6.5$). For large α , we observe a rapid fall in the effective mass around some critical value of the electron concentration (N_{sc}) above, which, however, the variation is extremely slow and is essentially linear. For example, for $\alpha = 5$, the effective mass drops by about two orders of magnitude at a critical concentration $N_{sc} \approx 3.6 \times 10^{12} \text{ cm}^{-2}$ beyond which the variation of m_F^* with N_s is not much appreciable. It is also observed that N_{sc} increases as α increases. For low α , say $\alpha = 1$, no such interesting behavior is observed. In Fig. 6, we show specifically how m_F^* varies with α for different values of N_s . One can observe that for a given electron concentration, there exists a critical coupling constant α_c below

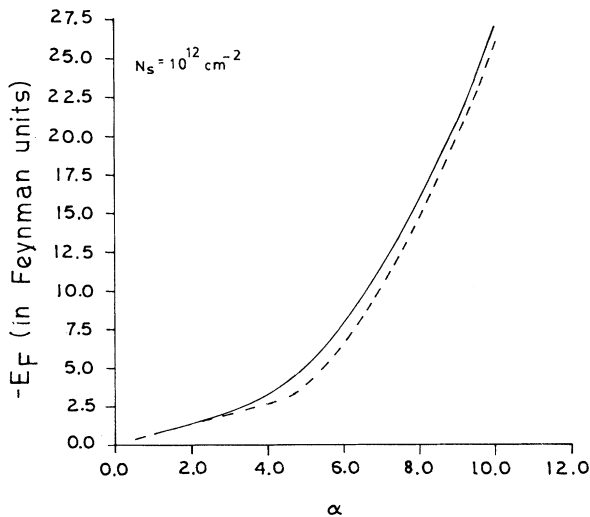


FIG. 3. $-E_F$ vs α , for $N_s = 10^{12} \text{ cm}^{-2}$; solid curve, FPIM result; dashed curve, LLP-H result.

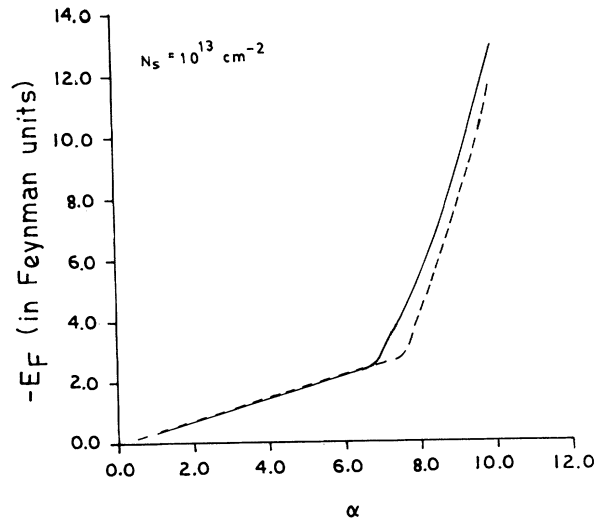


FIG. 4. $-E_F$ vs α , for $N_s = 10^{13} \text{ cm}^{-2}$; solid curve, FPIM result; dashed curve, LLP-H result.

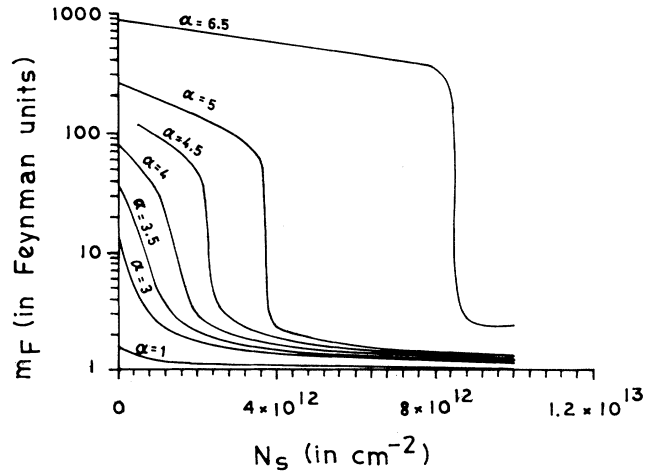


FIG. 5. Effective mass (m_F) vs N_s for $\alpha = 1, 3, 3.5, 4, 4.5, 5$, and 6.5 .

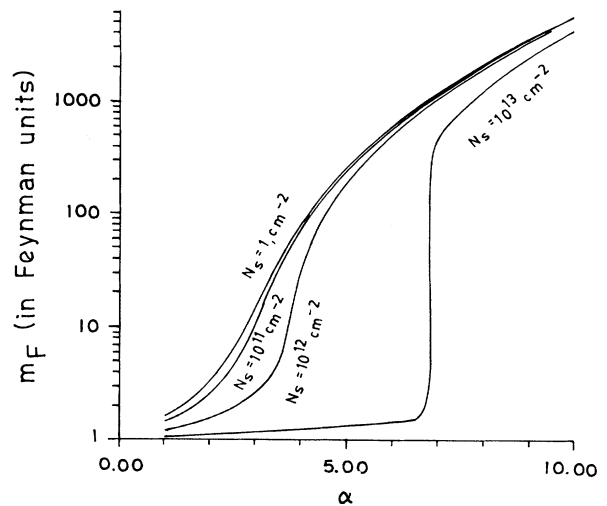


FIG. 6. m_F vs α , for $N_s = 1, 10^{11}, 10^{12}$, and 10^{13} cm^{-2} .

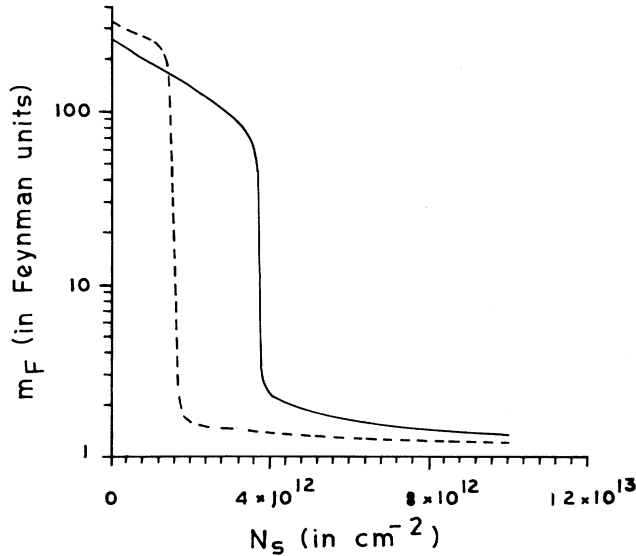


FIG. 7. m_F vs N_s for $\alpha=5$; Solid curve, FPIM result; dashed curve, LLP- H result.

which the effective mass is essentially linear in α and so the polaron should be in the weak-coupling phase and as the coupling constant exceeds α_c the effective mass increases rapidly indicating a strong-coupling phase. For large electron concentration the transition from the weak-coupling (or the delocalized) phase to the strong-coupling (or the localized) phase is very sharp as is seen for $N_s = 10^{13} \text{ cm}^{-2}$, whereas for low concentrations the transition may not be so sharp. In Fig. 7, we compare the effective-mass results obtained from FPIM with those calculated using the LLP- H method. We find that the value of N_{sc} obtained from FPIM is higher than that predicted from the LLP- H method. So we may conclude that the LLP- H method effectively overestimates the screening effect.

The existence of transition is also evident from the

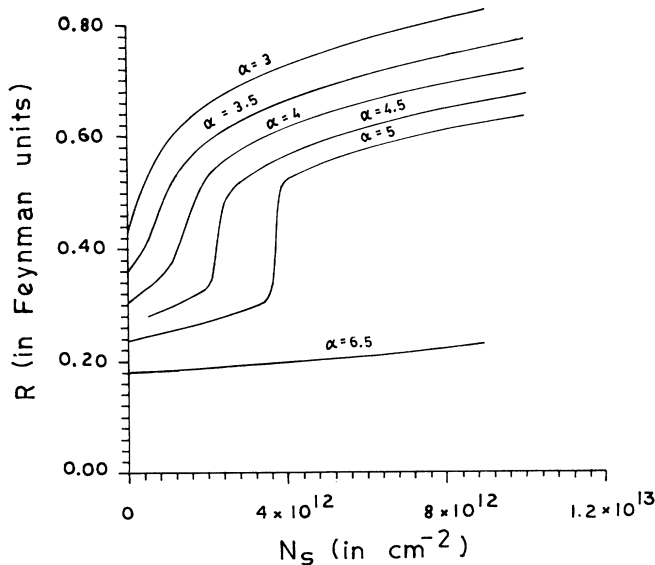


FIG. 8. Polaron size (R) vs N_s , for $\alpha=3, 3.5, 4, 4.5, 5$, and 6.5 .

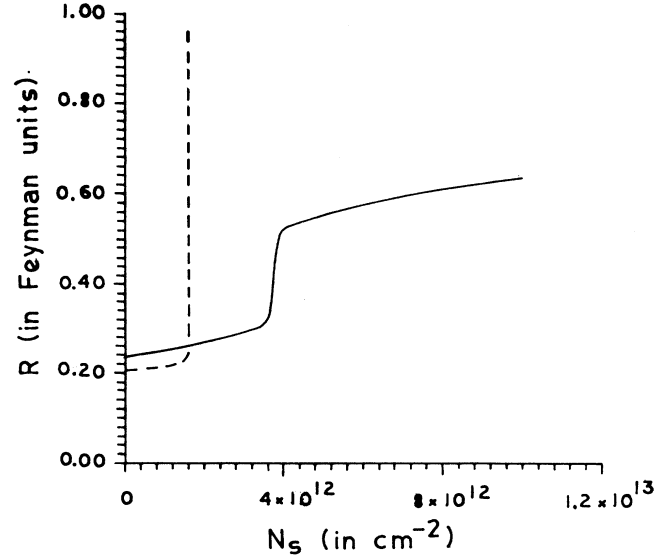


FIG. 9. R vs N_s for $\alpha=5$; solid curve, FPIM result; dashed curve, LLP- H result.

variation of the polaron size with N_s , which we plot in Fig. 8. For large values of α the polaron size shows a jump at $N_s = N_{sc}$. Again we see that N_{sc} increases with α . In Fig. 9, we compare the size of the polaron as obtained from FPIM with that predicted from the LLP- H method. According to the LLP- H method, the polaron is infinitely large in size in the entire weak-coupling phase which is a little unrealistic. This problem does not crop up in the FPIM solution which predicts only a finite jump in the polaron size at the transition point.

The explanation for the occurrence of the localization-delocalization transition discussed above is quite simple. It has been theoretically predicted that in a single polaron system, there exists a critical coupling constant at which the polaron should make a transition from the mobile state to a self-trapped state. Experimentally, however, it is difficult to verify this prediction because one cannot change the material parameters continuously to sweep the value of α around the critical value. In Ref. 6 and in the present paper, we have shown that one can change the effective coupling constant continuously by changing the electron density which is precisely the many-particle screening effect. As the electron density is increased, the electron-phonon interaction becomes more and more screened and at a sufficiently large carrier concentration, the interaction can become severely screened so that the effective coupling constant may reduce to a value which is equal to the single polaron critical coupling constant. At this value of the carrier density, we would expect the polaron to make a transition from the localized state to the delocalized state and such a transition should be observable in mobility and cyclotron resonance experiments.

IV. CONCLUSION

In conclusion, we have investigated the many-electron screening effect on the GS energy, effective mass and the

size of the polaron in a purely two dimensional polar semiconductor quantum well for the entire range of the coupling constant using the Feynman path-integral method and the static random-phase approximation. Comparison shows that the present results are qualitatively similar to those obtained earlier by us using the LLP- H variational method. Quantitatively, however, the present results are more reliable than the LLP- H results because mathematically FPIM is a more rigorous method and it provides a lower variational GS energy. We, therefore, reestablish our earlier conclusion that there exists a critical value of the carrier density (depending on the electron-phonon coupling constant) at which the polaron makes a transition from the self-trapped state to a delocalized state. For a material with a large value of α , this transition is expected to be quite sharp. This is an interesting theoretical observation and should be verified experimentally. One should look for this transition in mobility and cyclotron resonance experiments on inversion layers where the electron density can be varied almost continuously as is done in quantum Hall effect experiments. The potential materials which can show such transitions are clearly the ones with large electron-phonon coupling constants. Although a number of ionic crystals like alkali halides are known to have large coupling strengths,¹² most polar semiconductors available today are essentially weak-coupling systems. It is, however, known for the SiO₂-Si interface in metal-oxide-semiconductor field-effect transistor (MOSFET) that the polar nature of the interface phonons is due to the polar nature of SiO₂.¹³ Therefore, for the present purpose it will be desirable to fabricate a semiconductor-insulator interface in a MOSFET kind of device with the insulator

having a large electron-phonon coupling constant and the semiconductor having a small dielectric constant so that the coupling strength of the interface phonons to the electron in the inversion channel remains sufficiently large.

Finally, we would like to make a few remarks regarding our approximations. First, the use of the electron-gas dielectric function in the static RPA should not be rigorously valid in the self-trapped state because in this regime, the continuum approximation itself breaks down and, therefore, no analysis based on the Fröhlich model should be fully accurate. This, however, does not rule out the possibility of existence of the phase transition because the use of the electron-gas dielectric function is rigorously valid in the delocalized phase right up to the transition point. However, the static RPA might overestimate the screening effect because it does not take into account the effect of the exchange and correlation hole which exists around each electron. The effect of the exchange and correlation hole is to prevent other electrons from coming close to the one which participates in the dielectric screening. The present calculation can certainly be improved by using a better dielectric function such as the Hubbard dielectric function¹⁴ or the Singwi-Sjolander dielectric function,¹⁵ which will probably yield for the localization-delocalization transition higher critical densities than those obtained in the present work. We, however, believe that the improvement will be only marginal because the densities of interest in usual semiconductor quantum wells are orders of magnitude smaller than the metallic densities and, therefore, the higher-order correlation effects may not be all that important in the present problem.

¹M. Bhattacharya, A. Chatterjee, and T. K. Mitra, Phys. Rev. B **39**, 8351 (1989); Phys. Lett. A **134**, 391 (1989); S. Das Sarma, Phys. Rev. Lett. **52**, 859 (1984); S. Das Sarma and B. A. Mason, Ann. Phys. **163**, 78 (1985); F. M. Peeters, Wu Xiaoguang, and J. T. Devreese, Phys. Rev. B **34**, 1160 (1986); **37**, 933 (1988); S. W. Gu, X. J. Kong, and C. W. Wei, *ibid.* **36**, 7984 (1987); S. Sil and A. Chatterjee, J. Phys. Condens. Matter **3**, 9401 (1991); **5**, 1169 (1993); Int. J. Mod. Phys. B **7**, 4763 (1993).

²S. Das Sarma, Phys. Rev. B **27**, 2591 (1983).

³S. Das Sarma, Surf. Sci. **142**, 341 (1984); S. Das Sarma and B. A. Mason, Phys. Rev. B **31**, 5536 (1985); Wu Xiaoguang, F. M. Peeters, and J. T. Devreese, Phys. Status Solidi B **133**, 229 (1986); Phys. Rev. B **34**, 2621 (1986); **36**, 9765 (1987); S. P. Li and S. C. Wang, *ibid.* **40**, 1712 (1989); N. Mori, K. Taniguchi, C. Hamaguchi, and S. Hiyamizu, J. Phys. C **21**, 1791 (1988).

⁴G. Lindemann, W. Seidenbusch, R. Lassing, J. Edlinger, and E. Cornik, Physica B **117/118**, 649 (1983); D. C. Tsui, Th. Englert, A. Y. Cho, and A. C. Gossard, Phys. Rev. Lett. **44**, 341 (1980); G. Kido, N. Miura, H. Ono, and H. Sakaki, J. Phys.

Soc. Jpn. **51**, 2168 (1982); M. Horst, V. Menkt, and J. P. Kotthaus, Phys. Rev. Lett. **50**, 754 (1983); A. Pinczuk, M. G. Lamant, and A. C. Gossard, *ibid.*, **56**, 2902 (1986); G. Fasol, N. Mestres, H. P. Hughes, A. Fischer, and K. Ploog, *ibid.* **56**, 2216 (1986).

⁵H. Ehrenreich, J. Phys. Chem. Solids **8**, 130 (1959).

⁶A. Chatterjee and S. Sil, Solid State Commun. **87**, 329 (1993).

⁷W. J. Huybrechts, J. Phys. C **10**, 3761 (1977).

⁸T. D. Lee, F. Low, and D. Pines, Phys. Rev. **90**, 297 (1953).

⁹F. Stern, Phys. Rev. Lett. **18**, 547 (1967).

¹⁰R. Feynman, Phys. Rev. **97**, 660 (1950).

¹¹T. K. Mitra, A. Chatterjee, and S. Mukhopadhyay, Phys. Rep. **153**, 91 (1987).

¹²N. Tokuda, H. Shoji, and K. Yoneya, J. Phys. C **14**, 4281 (1981).

¹³F. Bechstedt and R. Enderlein, Phys. Status Solidi B **129**, 349 (1985).

¹⁴J. Hubbard, Proc. R. Soc. London Ser. A **243**, 336 (1957).

¹⁵P. Vashishta and K. S. Singwi, Phys. Rev. B **6**, 875 (1972).